J Mater Sci (2012) 47:892–897
DOI 10.1007/s10853-011-5869-x

Optical studies on lanthanum-doped calcium fluoride

C. Pandurangappa · B. N. Lakshminarasappa

Received: 4 June 2011 / Accepted: 10 August 2011 / Published online: 24 August 2011

Abstract Lanthanum-doped Calcium fluoride (CaF_2) nanoparticles were synthesized by co-precipitation method and characterized by powder X-ray diffraction, Fourier infrared spectroscopy (FTIR), Scanning electron microscopy (SEM), BET surface area measurements, and Optical absorption techniques. The X-ray diffraction pattern showed the cubic phase of fluorite structure. The average crystallite size was found to be ~25 nm. The FTIR spectrum showed the presence of hydroxyl groups in the as prepared sample with two strong IR absorption bands at ~3400 and 1550 cm^{-1}. The morphological features studied by SEM revealed that nanoparticles were agglomerated. Surface area measurements showed porous nature of the nanoparticles. The optical absorption spectrum of γ-irradiated samples showed a prominent absorption peak at ~385 nm and two weak ones at ~218 and 533 nm. The optical absorption was found to increase with increase in γ-dose.

Introduction

Nanophase materials are systems consisting of ultra fine particles having dimensions lying in the range of few nanometers to a few hundred nanometers. They generally include nanocrystalline thin films, sintered materials with ultra fine grain structure, and loosely aggregated nanoparticles. The physical properties such as structure, magnetic, optical, dielectric, thermal, electric, etc. of nanomaterials are very much affected from those of bulk materials due to their large surface to volume ratio and quantum confinement effects. Over the last decade, nanoparticles have attracted great interest and have become a research focus in terms of both their fundamental and technological importance [1]. This is particularly true in the case of luminescent materials since emission lifetime, luminescence quantum efficiency, and concentration quenching were found to strongly depend on the particle size in the nanometer range [2–4]. The manipulation of material properties will revolutionize the luminescence device area with huge advances in digital memory storage and optical resolution for image purposes, optical telecommunications, photonics, etc. High efficiencies [3], ultra-fast recombination times [5], interesting nonlinear optical behaviors [6], and unusual fluorescence were observed in nano crystals [7, 8]. Inorganic nanoparticles with controllable and uniform size and shape have attracted vast attention because of their unique size and shape-dependent properties and great potential applications. Formation of luminescent phosphor particles at nanoscale can change the structure, crystallinity, and optical properties of the host, thereby affecting the characteristics and efficiency of phosphor material. More attention has been given to search of new methods for synthesis of pure and doped nanomaterials.

Fluoride compounds are very attractive materials for many potential applications such as advanced phosphors, photonics, display monitors, imaging, light amplification, as well as precursors for transparent ceramics processing. Compared to oxide-based matrices, they present additional advantages such as a high transparency in a wide wavelength region from the VUV to the IR and a low phonon

C. Pandurangappa (✉)
Department of Physics, RNS Institute of Technology, Channasandra, Bangalore 560061, India
e-mail: cpandu@gmail.com

B. N. Lakshminarasappa
Department of Physics, Jnanabharathi Campus, Bangalore University, Bangalore 560056, India

energy that decreases the nonradiative transition probability of the active ions. However, there are limited reports on synthesis and characterization of rare earth-doped nanofluorides. Among the alkali fluoride compounds, calcium fluoride (CaF_2) is an attractive material because of its high stability and non-hygroscopic behavior. Recently, CaF_2 gained a renewed interest as a laser material when doped with rare earth material [9, 10]. However, reports on synthesis of La-doped CaF_2 nanoparticles and study of radiation-induced defects are very few. In this study, 2 mol% La-doped CaF_2 nanocrystals are synthesized by co-precipitation method and are characterized by XRD, SEM, FTIR, and Surface area. Also, radiation-induced defects in nanocrystalline CaF_2:La are identified by optical absorption technique.

Experimental

Synthesis

The starting ingredients for the synthesis nanocrystalline CaF_2:La were analar grade Calcium chloride ($CaCl_2$), Ammonium fluoride (NH_4F), Lanthanum nitrate $La(NO_3)_2$, and Ethanol. The flow chart for the co-precipitation synthesis of La-doped nanocrystalline CaF_2 is shown in Fig. 1. Stoichiometric quantities of $CaCl_2$, NH_4F, and $La(NO_3)_2$ were taken in a 250 mL conical flask and dissolved 100 mL of distilled water. The mixture was stirred for 2 h constantly to achieve homogeneity. During stirring, the transparent reaction mixture transforms into opaque white

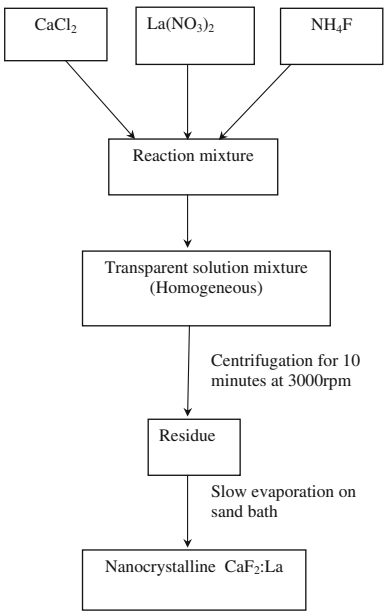

Fig. 1 Flow chart for synthesis of La-doped CaF_2 nanoparticles by co-precipitation method

suspension gradually. After 2 h stirring, the solution was centrifuged for 10 min at 3000 rpm using KEMI C8C Centrifuge and a white residue was obtained. The residue was washed thoroughly with ethanol to remove the residual chloride and the ammonium ions. The product was extracted on to a ceramic dish and dried slowly on a sand bath maintained at ~100 °C. The flow chart for the synthesis is shown in Fig. 1.

$$CaCl_2 + 2NH_4F + La(NO_3)_2 \rightarrow CaLaF_2 + 2NH_4NO_3 + Cl_2(g)$$

Characterization

The XRD measurements of synthesized samples were carried out using a Philips X-pert PRO powder diffractometer with Cu-K_α radiation ($\lambda = 1.54$ Å) in the scan range 10°–90°. The morphology of synthesized samples was studied using scanning electron microscopy (JEOL JLA-840A) by a sputtering technique with gold as covering contrast material. The FTIR spectrum was recorded using Nicolet Magna 550 spectrometer with KBr pellets in the range from 400 to 4000 cm^{-1}. The surface area and porosity of the synthesized samples were measured by Quantachrome Corporation, NOVA 1000 gas sorption analyzer. The samples were covered with black paper to prevent the entry of visible light into the sample. The γ-radiation of the pure and doped CaF_2 samples was carried out by exposing the samples to Co^{60} gamma chamber (supplied by Board of Radiation and Isotope Technology, Mumbai) with a dose rate of ~3.89 kGy per hour, installed at Health Physics Division, Indira Gandhi Center for Atomic Research (IGCAR), Kalpakkam, India. The γ-dose of the exposed CaF_2 samples was from 97.25 Gy to 15.56 KGy at room temperature (RT). The Optical absorption measurements of the samples were carried out in the wavelength range 200–900 nm using V-570 UV/VIS/NIR double beam spectrophotometer by dispersing the synthesized samples in liquid paraffin (nuzol).

Results and discussion

PXRD, SEM, and FTIR

Figure 2 shows the powder X-ray diffraction patterns (PXRD) of as prepared La-doped CaF_2. XRD peaks obtained are indexed and it results to cubic phase of the fluorite-type structure with space group Fm3m [11]. The pattern was compared with JCPDS Card no. 87–0971, and it is found to match well with those reported in the literature [12, 13]. The XRD patterns confirm the cubic crystallinity of synthesized nanoparticles. The observed peaks

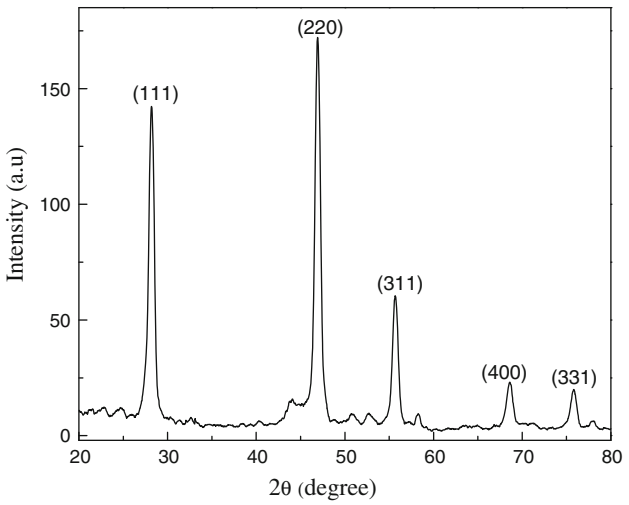

Fig. 2 Powder X-ray diffraction pattern of as-prepared La-doped CaF_2 nanoparticles

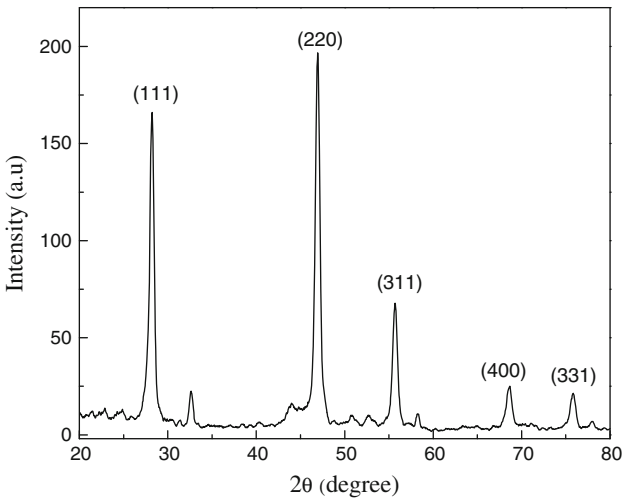

Fig. 3 Powder X-ray diffraction pattern of gamma-irradiated La-doped CaF_2 nanoparticles

correspond to <*h k l*> values of (1 1 1), (2 2 0), (3 1 1), (4 0 0), (3 1 1), and (4 2 2). Using the <*h k l*> values of different peaks, the lattice constant (a) of the sample was calculated. The average value of lattice constant was found to be 5.454 Å which is relatively more than that of undoped CaF_2 (5.435 Å, JCPDF 772096). This is due to the fact that when Ca^{2+} is substituted by a trivalent rare earth (La^{3+}) ion, charge balance compensating F^- ions enter the fluorite structure in interstitial fluoride cubic sites and the electronic repulsion between F^- ions leads to a net increase of the lattice parameter. The XRD pattern presents broad peaks revealing the small crystallite size of the synthesized samples. The crystallite size was calculated from the full width at half maximum (FWHM) technique using Scherer's formula $D = K\lambda/(\beta \cos\theta)$ where K is the constant (0.99), λ is the wavelength of Cu-Kα (1.54 Å) line, β is the FWHM, and θ is the diffraction angle. The average crystallite size of La-doped CaF_2 samples was found to be 25 nm. Figure 3 presents the powder XRD patterns of irradiated samples. Similar diffraction peaks were recorded at same 2θ positions. This indicates that irradiation does not reveal any structural changes in the nanocrystalline CaF_2. However, the intensity of peaks increased marginally and the peaks are sharp with relatively less width. The crystallite size was found to be increased to 30 nm. This indicates the agglomeration of nanoparticles due to irradiation.

Figure 4 shows the SEM photograph of as-prepared La-doped CaF_2 nanoparticles. The SEM results reveal that the powder was porous and agglomerated with polycrystalline nanoparticles. The larger particles exhibited numerous spherical perturbances on the surface, suggesting that they were formed during the precipitation process through fusion of smaller particles. The as-prepared products were found to

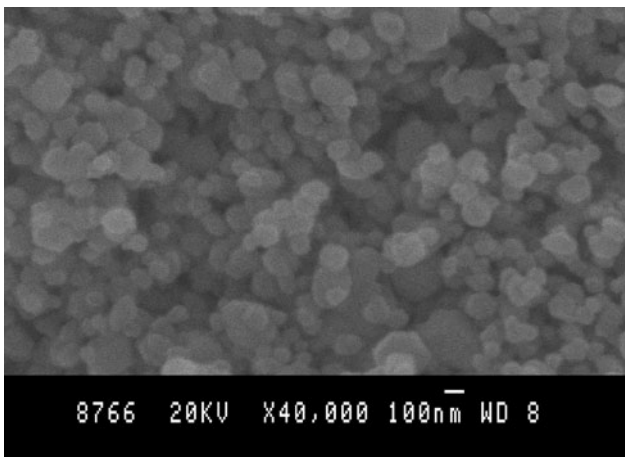

Fig. 4 Scanning Electron Microscope picture of as-prepared La-doped CaF_2 nanoparticles

have voids and were agglomerated from few microns to few tens of microns, fluffy and porous. The SEM of the irradiated samples showed larger particles than the as prepared one and indicated the agglomeration of the nanoparticles during irradiation (Fig. 5). FTIR absorption was measured to check the purity of the synthesized powder. Figure 6 shows the FTIR spectrum of as-prepared La-doped CaF_2 nanoparticles. The spectrum shows two strong IR absorption with peaks at 3446 and 1655 cm^{-1} which are the characteristic of H–O–H bending of the H_2O molecules revealing the presence hydroxyl groups in the as-prepared sample [14]. The fundamental frequency at $\sim$395 cm^{-1} arises due to hindered rotations of the hydroxyl ions. The band at $\sim$2368 cm^{-1} is due to KBr pellets used for recording FTIR spectrum. The irradiated samples showed less absorption (Fig. 7) for $\sim$3446 and 1655 cm^{-1} bands. This could be attributed to the release of water molecules trapped inside the solid matrix on

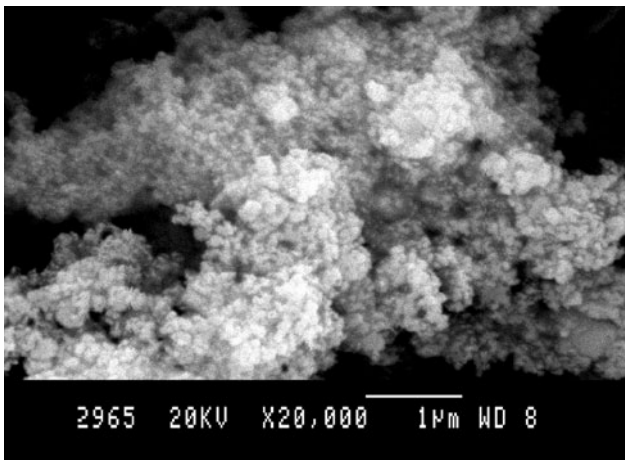

Fig. 5 Scanning Electron Microscope picture of gamma-irradiated La-doped CaF_2 nanoparticles

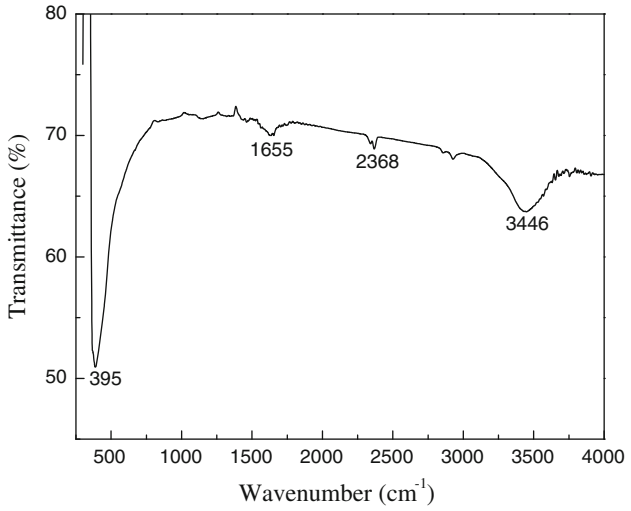

Fig. 6 Fourier Transform Infrared Spectrum of as prepared La-doped CaF_2 nanoparticles

irradiating the sample. The surface area of the CaF_2 samples was measured by BET method, and the obtained porosity values are shown in Table 1. Figures 8 and 9 represent the surface area plots of the CaF_2:La. The results are found to match well with literature [15]. It is observed that the surface area decreases significantly on irradiation of the samples by γ-rays.

Optical absorption

The optical absorption spectrum of pristine and γ-irradiated La-doped CaF_2 nanoparticles is shown in Fig. 10. It shows a prominent absorption peak at $\sim$385 nm and two weak absorptions at $\sim$218 and 533 nm. The intensity of absorption was found to increase with increase in γ-dose. However, the pristine sample did not show any absorption. The band at

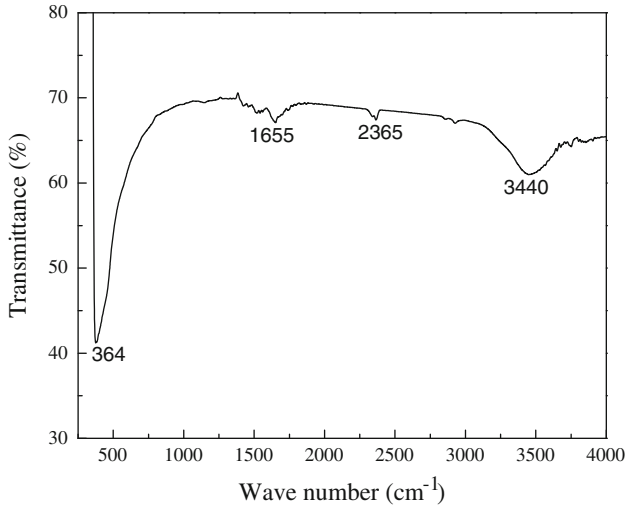

Fig. 7 Fourier Transform Infrared Spectrum of gamma-irradiated La-doped CaF_2 nanoparticles

Table 1 Surface area, pore volume, and pore diameter of CaF_2

Compound	Surface area (m^2/g)	Average pore diameter (Å)	Total pore volume (cc/g)	BET *C*
La-doped CaF_2	32.254	55.678	0.05233	45.7632
Heat-treated CaF_2:La	16.3735	46.352	0.01234	134.876

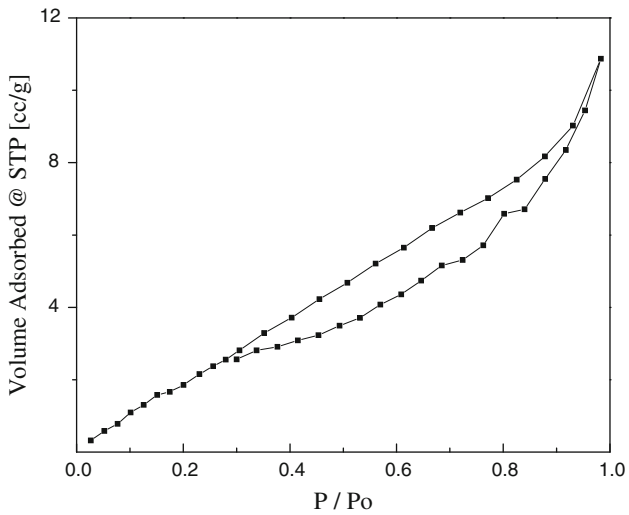

Fig. 8 Pore size distribution of as-prepared La-doped CaF_2 nanoparticles

$\sim$218 nm is a characteristic absorption of CaF_2. It is well established that nanomaterials have large surface to volume ratio. This results in the formation of voids on the surface as well inside the agglomerated nanoparticles. Such voids can cause fundamental absorption in the UV wavelength range

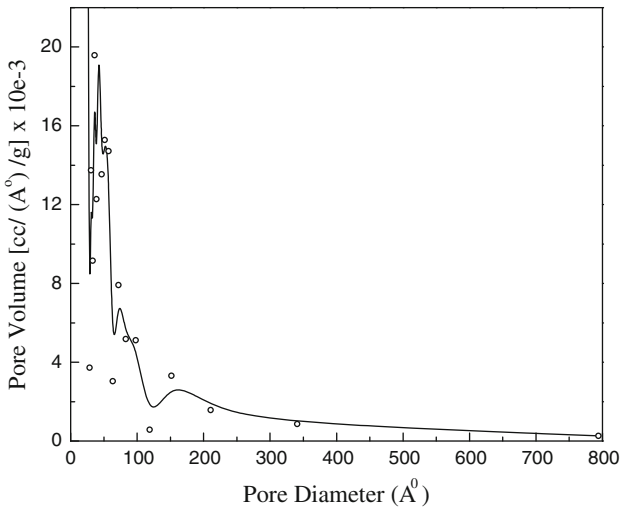

Fig. 9 N_2 adsorption–desorption isotherms of as-prepared La-doped CaF_2 nanoparticles

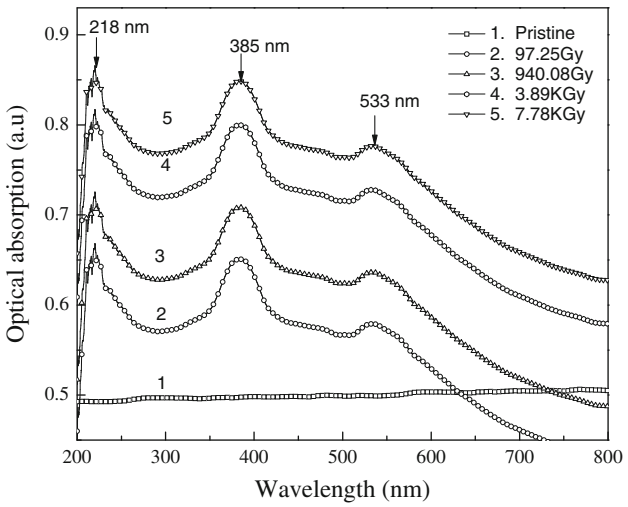

Fig. 10 Optical absorption spectrum of pristine and gamma-irradiated La-doped CaF_2 nanoparticles

[16]. Also, surfaces of nanoparticles are well known to comprise of several defects such as dangling bonds, regions of disorder, and adsorption of impurity species which result in optical absorption of nanocrystals. It is reported that the fluorine (F^-) ions interstitials lead to a dominant defect structure [17]. Also defects in the rare earth-doped CaF_2 can aggregate and form clusters which have an effect on nanoparticles growth. Smaller size nanoparticles of ~10–20 nm have high surface to volume ratio which results in increase of defects distribution on the surface of nanomaterials. Thus, the absorption band at 218 nm in this study may be attributed to surface defects in nanocrystalline CaF_2:La.

Literature reports that Staebler and Schnatterly [18] observed absorption peaks at ~270, 410, and 620 nm in the additively colored La-doped CaF_2 single crystals. They attributed 410 nm band to photo chromatic center. It is proved that additive coloration or gamma irradiation of La-doped CaF_2 single crystals exhibit photochromic effect. It is a process in which the color of the samples is changed upon to their radiations. The effect is ascribed to a photoreversible electron transfer between the La ions and photochromic color center produced during irradiation. Absorption of UV light by the photochromic center transfers an electron to an isolated La^{3+} ion. The process is reversible by absorption of visible light by La^{2+}. Philips and Duncan [19] have proved the existence of photochromic centers in gamma-irradiated lanthanum-doped CaF_2 single crystals by bleaching experiments. The 620 nm band is attributed to reduction of the trivalent La ions to divalent state. Literature reveals that in lanthanum-doped the La ions exist in La^{3+} state. Merz and Pershan [20] and de Melo et al. [21] proved that in lanthanum-doped CaF_2, La ions exist in La^{3+} state. They proposed that during gamma irradiation electrons and holes are generated in lattice of CaF_2. The La^{3+} ion captures the released electron and gets reduce to La^{2+} state. Sunta [22] proposed a model in support the above mechanism. Hayes and Twidell [23] have proved through EPR experiments that La^{2+} ions in CaF_2 are stable at RT for a period of few days and gradually decay to the trivalent state at RT.

The 385 nm absorption peak in this study is attributed to F-center. γ-irradiation produces free electrons which will be trapped at negative ion vacancies and form the F-centers. It is known that if alkaline earth fluoride crystals such as CaF_2 are γ-irradiated for prolonged times of a few hours, F-centers are formed at RT [24]. The absorption peak at 533 nm is attributed to Ca colloids formed during irradiation. It is reported that in calcium fluoride, the aggregation of point defects produced by energetic radiation form colloids [25]. They absorb strongly in the 530–600 nm region with a spectrum that depends on particle size.

Conclusions

Lanthanum-doped CaF_2 nanoparticles were synthesized successfully by co-precipitation method and characterized by XRD, SEM, and FTIR. The average particle size of the synthesized samples was found to be 25 nm. The morphological features showed that the as-prepared samples were agglomerated from few microns to a few tens of microns, fluffy and porous. The FTIR spectrum revealed the presence of hydroxyl groups in the as-prepared sample. The gamma irradiation of samples is found to increase the particle size marginally. The optical absorption spectra showed the presence of radiation-induced defects in the irradiated nanocrystalline samples.

References

1. Ratner M, Ratner D (2003) Nano Technology. Pearson Pte Ltd, Indian Branch, Delhi
2. Rodríguez J, García MF (2007) Synthesis, properties and applications of oxide nanomaterials. Wiley-Interscience, New Jersey
3. Rao CNR, Muller A, Cheetham AK (2007) Nanomaterials chemistry—recent developments and new directions. Wiley-Interscience, New Jersey
4. Blasse G, Grabmaier BC (1994) Luminescent materials. Springer-Verlag, Berlin
5. Kenyon AJ (2002) Prog Quantum Electron 26:225
6. Peng X, Schlamp MC, Kadavanich AV, Alivisatos AP (1997) J Am Chem Soc 119:7019
7. Counio G, Gacoin T, Boilot JP (1998) J Phys Chem B 102:5257
8. Justel T, Nikol Ronda H, Angew C (1998) Chem Int Ed 22:3085
9. Petit V, Doualan JL, Camy P, Menard V, Moncorge R (2004) Appl Phys B 78:681
10. Luccas A, Debourg G, Jacquemet M, Druon F, Balembois F, Georges P, Camy P, Doualn JL, Moncorge R (2004) Opt Lett 29:2767
11. Sun X, Li U (2003) Chem Commun 14:1768
12. Fujihara S, Kadota Y, Kimura T (2002) J Sol-Gel Sci Technol 24:147
13. Hong BC, Kawano K (2006) J Alloys Compd 408–412:838
14. Bensalah A, Mortier M, Patriarcheb G, Gredin P, Vivien D (2006) J Solid State Chem 179:2636
15. Sun L, Chow LC (2008) Dent Mater 24(1):111
16. Kumar GA, Chen CW, Ballato J, Riman RE (2007) Chem Mater 19:1523
17. Aubry P, Bensalah A, Gredin P, Patriarche G, Vivien D, Mortier M (2009) Opt Mater 31:750
18. Staebler, Schnatterly (1971) Phys Rev B 2:516
19. Philips W, Duncan RC Jr (1971) Metall Mater Trans 2:769
20. Merz L, Pershan PS (1967) Phys Rev 162:217
21. de Melo AP, de Lima JF, Figueredo AMG, Chadwick AV, Valerio MEG (1997) Mater Sci Forum 239–241:749
22. Sunta CM (1985) Nucl Tracks 10:47
23. Hayes W, Twidell JW (1963) Proc Phys. Soc 82:330
24. Dantas NO, Watanabe S, Chubaci JFD (1996) Nucl Instrum Methods Phys Res B 116:269
25. Cramer LP, Langford SC, Dickinson JT (2006) J Appl Phys 99:054305